



HAL
open science

Comprehensive evaluation of collaborative filtering in drug repurposing

Clémence Réda, Jill-Jênn Vie, Olaf Wolkenhauer

► **To cite this version:**

Clémence Réda, Jill-Jênn Vie, Olaf Wolkenhauer. Comprehensive evaluation of collaborative filtering in drug repurposing. 2024. hal-04626970

HAL Id: hal-04626970

<https://hal.science/hal-04626970>

Preprint submitted on 27 Jun 2024

HAL is a multi-disciplinary open access archive for the deposit and dissemination of scientific research documents, whether they are published or not. The documents may come from teaching and research institutions in France or abroad, or from public or private research centers.

L'archive ouverte pluridisciplinaire **HAL**, est destinée au dépôt et à la diffusion de documents scientifiques de niveau recherche, publiés ou non, émanant des établissements d'enseignement et de recherche français ou étrangers, des laboratoires publics ou privés.



Distributed under a Creative Commons Attribution - NonCommercial - NoDerivatives 4.0 International License

Comprehensive evaluation of collaborative filtering in drug repurposing

Clémence Réda*

ORCID: 0000-0003-3238-0258

Department of Systems Biology and Bioinformatics, University of Rostock,
G-18051 Rostock, Germany
clemence.reda@uni-rostock.de

* Corresponding author

Jill-Jénn Vie

ORCID: 0000-0002-9304-2220

Soda Team, Inria Saclay,
F-91120 Palaiseau, France
jill-jenn.vie@inria.fr

Olaf Wolkenhauer

ORCID: 0000-0001-6105-2937

Dept of Systems Biology & Bioinformatics, University of Rostock, 18051 Rostock, Germany
Leibniz-Institute for Food Systems Biology, Freising, 85354, Germany
Stellenbosch Institute of Advanced Study, Wallenberg Research Centre
Stellenbosch, SA-7602, South Africa
olaf.wolkenhauer@uni-rostock.de

Abstract

Drug development is known to be a costly and time-consuming process, which is prone to high failure rates. Drug repurposing allows drug discovery to consider reusing approved compounds to mitigate those issues. The outcomes of past clinical trials can be used to predict novel drug-disease associations by leveraging drug- and disease-related similarities. To tackle this classification problem, collaborative filtering with implicit feedback has become popular. It can handle large imbalances between negative and positive known associations and known and unknown associations. However, properly evaluating the improvement over the state of the art is challenging, as there is no consensus approach to compare models. We propose a reproducible methodology for comparing collaborative filtering-based drug repurposing. We illustrate this method by comparing 11 models from the literature on eight diverse drug repurposing datasets. Based on this benchmark, we derive guidelines to ensure a fair and comprehensive evaluation of the performance of those models. Those contributions constitute an essential step towards increased reproducibility and more accessible development of competitive drug repurposing methods.

Keywords Drug repositioning, Drug repurposing, Collaborative filtering, Benchmark, Matrix factorization

1 Introduction

Developing novel drugs has turned out to be a long, expensive, and strict process. The time window between identifying a drug candidate and its marketing is around 5 years, but it can take up to 10 years and cost an average of \$2.3 billion [38]. Still, the failure rate in commercializing a candidate drug is up to 90% [50]. This has led researchers to consider already well-understood drugs instead of *de novo* drug designs.

Drug repurposing aims to screen large libraries of well-documented chemical compounds in an automated fashion to uncover new drug-disease associations. In the light of large available amounts of heterogeneous clinical data (with several public databases storing data, *e.g.*, for omics data from drug perturbations [49], drug sensitivities [58], or clinical trial results [63]), and increased computational power, this type of approach becomes more and more attractive. The underlying hypothesis behind drug repurposing is that drugs might target multiple biological processes in which dysregulations are causal factors accounting for a given pathology. Diseases might share those dysregulations [19]. Moreover, since drug discovery is restricted to approved molecules, drug repurposing speeds up the early preclinical phases and toxicity analyses in the pipeline. Focusing on well-known

molecules, in turn, avoids the emergence of unexpected adverse side effects at late development stages, which still constitute one of the main reasons for marketing failure in late clinical phases [17].

Several approaches to drug repurposing have been developed in the literature. We refer to [18, 39] for a comprehensive overview of those methods. In drug repurposing, a classifier can be trained to match and predict outcomes from past clinical trials, as made available by ClinicalTrials.gov [63], or the RepoDB database [7] for instance. Such a classifier might be based on relevant biological features of drugs and diseases or rely solely on the reported clinical trial outcomes. Those outcomes are known to be highly imbalanced between positive and negative outcomes because negative results are rarely reported [23, 6]. Those adverse outcomes might result from late discovery toxicity effects or low accrual. Moreover, the number of untested drug-disease associations dramatically outnumbers the number of past clinical trials. For example, in the TRANSCRIPT [42] and PREDICT [41] datasets which were published last year, the ratio between negative and positive drug-disease matches is around 3%. In contrast, the sparsity number—the percentage of unknown matches over the total number of possible matches—is larger than 98.5%. Attempting to overcome this lack of data by considering all unknown outcomes as negative, as tempting as it may be, might induce considerable bias in the underlying model. Indeed, a drug-disease association might not have been tested for various reasons, including the incompleteness of knowledge on biological events. This might explain that binary classifiers fail on not fully annotated datasets [36]. Moreover, another reason untested drug-disease pairs cannot be considered fully-fledged negative results is that one is looking for novel drug indications among these pairs. Nonetheless, the fact that a drug-disease association has not been tested is already informative. This type of implicit information (often named *implicit feedback*) arises in many other non-medical topics of recommendation, for instance advertising [48].

Collaborative filtering is a flexible semi-supervised approach that has raised a lot of interest in the domain of recommendation systems. This framework has also become popular in drug repurposing, considering drugs as items and diseases as users [61, 57], notably thanks to the Netflix Prize problem [51], which aimed to connect movies and viewers. Predicted drug-disease associations stem from a function whose parameters are learned on a whole matrix of drug-disease matches instead of focusing on a single disease at a time. Then, such methods rely on filtering patterns learned across diseases and drugs, implementing some collaboration (see Figure 1 for an illustration of this principle). A few examples of simple collaborative filtering methods are nearest neighbor approaches, where an outcome is assigned to a pair based on a consensus on similar datapoints [11], and matrix factorization, in which literature often relies on tensor decomposition, *i.e.*, any drug-disease matching in the matrix is the output of a classifier in which only lower-rank tensors intervene. This principle is present, for instance, in factorization machines [45].

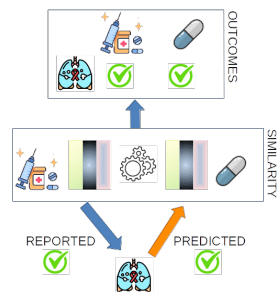


Figure 1: Principle of collaborative filtering. If two drugs A and B are similar, and if there is a known association between a disease and drug A, then the same association is predicted between this disease and drug B.

Although the application of collaborative filtering to drug repurposing has become increasingly popular in the last ten years [48, 61, 57, 29, 16, 59, 60, 30], the field lacks a standard benchmark approach to evaluate the performance of new algorithms. Across papers, several different metrics, datasets, and baseline algorithms have been selected, undermining the comparability and application of the proposed methods. Due to the hurdles in running the methods and accessing drug repurposing datasets, numerical results from baseline algorithms are sometimes copied directly from the original paper. Moreover, reproducibility issues specific to the implementation of the experiments further undermine the experimental results: for instance, not setting a fixed random seed, varying number of iterations, lack of package versioning, and differences in hyperparameter tuning. As a general rule, such a reproducibility issue is still pervasive in machine learning, as raised by several papers [34, 1, 24]. Conversely, the tremendous progress in computer vision and large language models (LLMs), for instance, has been credited to constructing standard datasets and benchmarks in those fields [15, 25].

Contributions **1.** To bridge that gap in the literature, we performed a benchmark across 11 published and open-access drug repurposing approaches based on collaborative filtering (see Table 2) on eight different drug repurposing datasets and a synthetic one (see Table 1). The algorithms and the datasets are available *via* two recently published open-source Python packages [44]. **2.** This large-scale benchmark allowed us to suggest guidelines for performing a fair and comprehensive assessment of those methods applied to drug repurposing. In particular, the dataset selection, the validation metric, and the split into training and testing sets are crucial to a benchmark. **3.** We show that methods relying on constructing a heterogeneous graph connecting drugs and diseases usually perform best in this benchmark. This result will hopefully support the faster development of novel approaches to drug repurposing, especially regarding interpretability.

In Section 2, we formally define the drug repurposing problem in a collaborative filtering framework and suggest a classification of state-of-the-art algorithms that tackle this problem. In Section 5, we describe the methodology behind our benchmark, along with the selected algorithms and datasets. Section 3 displays our benchmark results, that is, the ranking of the considered state-of-the-art algorithms and the experiments specific to the choice of a dataset and a validation metric. Finally, we discuss the impact of our research in Section 4.

Type	Dataset	Paper	N_S	F_S	N_P	F_P	#Positive	#Negative	s (%)	IR (%)	
Text-mining	Cdataset	[32]	663	663	409	409	2,532	0	99.1	0	
	Fdataset	[13, 32]	593	593	313	313	1,933	0	99.0	0	
	DNdataset	[33]	550	1,490	360	4,516	1,008	0	99.5	0	
Biological	Gottlieb	[13, 12]	593	1,779	313	313	1,933	0	99.0	0	
	LRSSL	[27]	763	2,049	681	681	3,051	0	99.4	0	
	(private)	PREDICT	[41]	1,351	6,265	1,066	2,914	5,624	152	99.6	2.70
	(public)	PREDICT	[41]	1,014	1,642	941	1,490	4,627	132	99.5	2.85
		TRANSCRIPT	[42]	204	12,096	116	12,096	401	11	98.3	2.74
Artificial	Synthetic	[43]	300	25	300	25	200	100	99.7	50	

Table 1: Datasets in the benchmark. They correspond to the number of drugs and diseases involved in at least one nonzero drug-disease association. The sparsity s is the percentage of unknown (neither positive nor negative) matches times 100 over the total number of possible drug-disease matches (rounded up to the first decimal place). The imbalance ratio **IR** is the ratio between negative and positive outcomes in the dataset (rounded up to the second decimal place). The private version of PREDICT is the one generated from notebooks in the original GitHub repository, whereas the public one is the one deposited on Zenodo [41]. The association matrix in the Fdataset comes from [13]. Still, the drug and disease features are from [32].

2 Problem statement

Part of our contribution to this work is an overview of state-of-the-art approaches to collaborative filtering, especially in drug repurposing. We also provide insights into applying these algorithms for medical and biological research.

2.1 The drug repurposing problem

A drug repurposing dataset first comprises a drug-disease association matrix denoted $A \in \{-1, 0, +1\}^{N_S \times N_P}$, which summarizes all known matches between chemical compounds and pathologies. N_S is the number of drugs, and N_P is the number of diseases for which at least one matching with a disease/drug is known. That is, every row and every column in matrix A has at least one non-zero coefficient. 0 means that the drug-disease association is deemed unknown (for instance, no Phase III clinical trial testing of this association has been reported). +1 means that the drug is efficient in treating the disease, for instance, through a successful clinical trial. -1 means that matching the drug and the disease is not recommended. Notably, until recently, no drug repurposing datasets featured negative associations (see Table 1) due to the difficulty in defining a negative association, and only comprise positive or unknown associations. In the remainder of this paper, similarly to a prior work [44], we define a negative drug-disease association as a drug-disease pair where either the drug is too toxic or too inefficient (*e.g.*, linked to reported low accrual in clinical trials). We expect those explicit negative annotations to improve the performance of a drug repurposing classifier outputting labels in $\{-1, +1\}$. How to take into account negative examples is still the subject of recent theoretical works on collaborative filtering [21], but it has not been tackled in the applications to drug repurposing. Ultimately, collaborative filtering aims to replace zeroes in matrix A by values in $\{-1, +1\}$. In the remainder of the paper, we denote $\hat{R} \in \mathbb{R}^{N_S \times N_P}$ the predicted association score matrix.

In addition to the association matrix A , some information about the drugs and diseases is also available to define drug and disease similarities. Different data types are featured in currently available drug repurposing datasets, as shown in Table 1. Drug and disease feature information is very heterogeneous: for instance, the Cdataset, the Fdataset [32], and the DNdataset [33] rely on text-mining approaches. More specifically, the drug-disease associations are first mined from the DrugBank [56] database. Then, for the Cdataset and Fdataset, the drug information S corresponds to Tanimoto drug similarity scores computed on 2D fingerprints of chemical structures. In contrast, disease features in P are a disease similarity matrix computed on their respective medical descriptions in OMIM [14]. In DNdataset, the drug similarity matrix S is computed using Lin’s node-based similarity function [28] on the anatomical therapeutic chemical (ATC) codes for drugs. Lin’s node-based similarity is also applied to disease ontologies [47] for the disease similarity matrix P . Note that those similarities are computed on a set of drugs and diseases larger than the number of entities involved in at least one non-zero association.

Recently, some works proposed biological data-based datasets for collaborative filtering-based drug repurposing. In the LRSSL dataset [27], drug features include the binary fingerprints of chemical structures and target protein domains and disease features are disease semantic similarities based on the intersection between disease-specific directed acyclic graphs of descriptors [53]. Similarly, the Gottlieb dataset [12] comprise drug-pairwise chemical, domain, functional (as Jaccard scores computed on Gene Ontology [2]) and disease semantic similarity matrices on drugs and diseases present in the associations in Fdataset. Those similarity matrices are concatenated in Table 1. The PREDICT [41] dataset incorporates several types of drug and disease

Class of algorithms	Name	Paper	I/O type	Use of features	Implementation
Matrix Factorization	ALS-WR	[4]	Matrix	×	Python
	LibMF	[9]	Matrix	×	Python
	LogisticMF	[22]	Matrix	×	Python
	PMF	[46]	Matrix	×	Python
	SCPMF	[35]	Matrix	×	MATLAB / Octave
Neural Network	Fast.ai collab_learner	[20]	Pair	×	Python
	NIMCGCN	[26]	Pair	✓	Python
Graph-Based	BNNR	[57]	Matrix	✓	MATLAB / Octave
	DRRS	[31]	Matrix	✓	MATLAB Compiler
	HAN	[54]	Pair	✓	Python
	LRSSL	[27]	Pair	✓	R

Table 2: Overview of algorithms present in the benchmark present in Section 5 and the classification (columns “Class” and “I/O type”) defined in Section 2.

similarity measures based on disease phenotypes, drug chemical structures, target gene proximity in a protein-protein interaction network, etc., similar to what was described in the seminal paper of the PREDICT method [13]. Finally, the TRANSCRIPT [42] dataset only includes transcriptomic-related data, as the drug and disease features are variations of gene-wise transcriptomic levels induced by the corresponding treatment/pathology, computed by performing a differential analysis on relevant samples from the LINCS L1000 database [49] (for drugs) or retrieved from the CREEDS database [55] (for diseases and drugs missing from LINCS L1000). Note that the code that generated both datasets is open-source [40].

All of that drug (resp., disease)-related information is summarized in a drug and a disease feature matrices $S \in \mathbb{R}^{N_S \times F_S}$ and $P \in \mathbb{R}^{N_P \times F_P}$. F_S is the number of drug features (e.g., genes when considering gene expression data, drugs when S is a similarity matrix), and analogously, F_P is the number of disease features. When not considering features, collaborative filtering relies on drug-drug and disease-disease similarities by comparing rows and columns of matrix A . For instance, if drug d is associated with row $r_d = [+1, 0, +1, -1]$ in matrix A , and drug d' with row $r_{d'} = [+1, +1, +1, -1]$, then we can possibly set the second coefficient of r_d to $+1$. Note that we ignore in this work the impact of missing and non-finite values on classification, e.g., $S \in (\mathbb{R} \cup \{\pm \text{inf}, \text{N/A}\})^{N_S \times F_S}$, which is in practice extremely relevant when dealing with real-life data. See Section 5 for the processing of non-finite data.

2.2 Classification of collaborative filtering algorithms

Based on our review of the literature in the domain in Table 2, we define three large classes of algorithms that depend on the underlying mechanism of repurposing.

Matrix factorization algorithms typically ignore side information from matrices S and P and aim to infer low-rank tensors such that a function of their product is as close as possible to matrix A . As such, these algorithms take the incomplete association matrix A as primary input and output the “completed” matrix $\hat{R} \in \mathbb{R}^{N_S \times N_P}$ which should match A on its known coefficients. High scores in \hat{R} should match positive coefficients in A , and conversely, low scores should correspond to negative or null values in A . Predictions on unknown drug-disease matches are made by setting a threshold t on the scores, such that drug-disease pair (i, j) is a positive association if and only if $\hat{R}_{i,j} > t$.

Neural networks are versatile algorithms that can be applied to classification. Given a set of weights θ , a neural network f defines the outcome associated with a feature vector x of a drug-disease pair by $f_\theta(x) \in \mathbb{R}$. Again, such outcomes should match the values in A . One might obtain true labels either by a thresholding approach or by adding a last softmax layer to the network and outputting the class associated with the highest score. However, contrary to most matrix factorization approaches, neural networks are a flexible way to integrate supplementary information about drugs and diseases in matrices S and P or to learn embeddings of drugs and diseases based on shared matches.

Finally, we define a third, less obvious class of algorithms called “graph-based”. Albeit they might rely to some extent on neural networks and tensor factorization, they are characterized by their building of a heterogenous (not necessarily bipartite) graph connecting drugs and diseases. Often, the edges of this graph can be split into three main groups: edges connecting a pair of drugs, a pair of diseases, or a drug and a disease. Drug repurposing aims to reconstruct edges from the last set, but a critical side advantage of those algorithms is to retrieve similarities between drugs and diseases. In particular, such edges might be helpful to justify predicted drug-disease associations and contribute to the interpretability of classifiers. This algorithm can either output pair-related scores or a full association matrix (see Table 2).

Type	Metric	Notation	Formula
Global	Accuracy	$\text{Acc}(\hat{R}, A; t)$	$(\Omega^- + \Omega^+)^{-1} \sum_{(i,j) \in \Omega^- \cup \Omega^+} \mathbb{1}((\hat{R}[i, j] - t)A[i, j] > 0)$
	Area Under the Curve	$\text{AUC}(\hat{R}, A)$	$\int_0^1 \text{TPR}(\text{FPR}^{-1}(x; \hat{R}, A); \hat{R}, A) dx$
Local	Average AUC	$\text{AUC}_d(\hat{R}, A)$	$N_P^{-1} \sum_{j \leq N_P} \text{AUC}(\hat{R}[\cdot, j], A[\cdot, j])$
	Average NS-AUC [62]	$\text{NS-AUC}(\hat{R}, A)$	$ N_P ^{-1} \sum_{j \leq N_P} \tilde{\Omega}_j ^{-1} \sum_{(i,i') \in \tilde{\Omega}_j} \mathbb{1}(\hat{R}[i, j] > \hat{R}[i', j])$
	Average NDCG@ N_S	$\text{NDCG}(\hat{R}, A)$	$N_P^{-1} \sum_{j \leq N_P} \left(\sum_{i=1}^{N_S^+} \frac{A[\sigma_{\hat{R}[\cdot, j]}(i), j]}{\log_2(i+1)} \right) / \left(\sum_{i=1}^{N_S^+} \frac{1}{\log_2(i+1)} \right)$

Table 3: Description of the considered validation metrics present in Section 5. $\Omega^\pm \triangleq \{(i, j), A[i, j] = \pm 1 \mid i \leq N_S, j \leq N_P\}$, whereas $\Omega_j^+ \triangleq \{i \mid A[i, j] = +1\}$ and $\tilde{\Omega}_j \triangleq \{(i, i') \mid A[i, j] > A[i', j]\}$ for any $j \leq N_P$. In the benchmark, $t = 0$ and $\mathbb{1}(C)$ is equal to 1 if C is satisfied, 0 otherwise. σ_V is the permutation that sorts all coefficients of any vector V of length n in decreasing order, that is, $V[\sigma_V(1)] \geq V[\sigma_V(2)] \geq \dots \geq V[\sigma_V(n)]$. The true positive rate is defined as $\text{TPR}(t; \hat{R}, A) = \sum_{(i,j), A[i,j]=+1} \mathbb{1}(\hat{R}_{i,j} > t) / \sum_{(i,j)} \mathbb{1}(\hat{R}_{i,j} > t)$ and $\text{FPR}(t; \hat{R}, A) = \sum_{(i,j), A[i,j]=-1} \mathbb{1}(\hat{R}_{i,j} > t) / \sum_{(i,j)} \mathbb{1}(\hat{R}_{i,j} \leq t)$ is the false positive rate. Finally, N_S^+ is defined as $\min(N_S, |\Omega_j^+|)$.

2.3 Pairs or matrices?

In addition to the three classes of algorithms defined in the last paragraph, state-of-the-art algorithms can also be discriminated by the type of their input/output (column “I/O type” in Table 2). In particular, those algorithms receive and output either a drug-disease association matrix or a drug-disease pair. We emphasize that choosing one type of algorithm or the other considerably impacts the resulting repurposing, both at training and prediction times. We would not recommend using matrix-oriented methods in drug repurposing.

Indeed, at training/testing time, when run on a subset of a drug repurposing dataset, algorithms that take as input an entire matrix cannot distinguish between “accessible” zeroes of the association matrix (*i.e.*, zeroes in the whole, initial, drug repurposing dataset) and “inaccessible” zeroes (that is, drug-disease matches which are masked in the subset but are non-zero coefficients in the full dataset). This simultaneously leads to data leakage and corrupted validation.

The data leakage stems from the fact that, in that case, an unknown drug-disease matching can never be hidden in the training set, as there is no mechanism to encode “inaccessible” *true* zeroes in the association matrix. As such, the algorithm is trained on information that is supposed to be accessible only at testing time. An approach to avoid this would be to ensure all zeroes in the initial association matrix A belong to the training set and none belong to the validation subset. Then, the chosen accuracy metric would be computed only on non-zero elements of the validation subset. Since most drug repurposing datasets only feature 0-1 values (and none of the true negatives denoted by -1 ’s), most standard metrics cannot be computed, as they require at least two types of labels. That metric type notably includes the popular Area Under the Curve (AUC). Note that, given the (very) low number of negative drug-disease associations in Table 1, restricting the training to datasets involving at least one negative example would inevitably lead to overfitting, which is, of course, undesirable. This problem of data leakage cannot then be fixed and might, unfortunately, account for the apparent good results of matrix-oriented approaches in our benchmark (see Section 3).

The corrupted validation comes from an incorrect implementation of the validation procedure, which is present in papers mentioning matrix-oriented approaches for drug repurposing and publishing code for their experiments. Indeed, if the selected accuracy/validation metric is computed across all coefficients/labels of matrix \hat{R} —regardless of the accessibility of the coefficients at training time—this metric might be inflated by the values obtained on unknown drug-disease pairs. This issue was solved during the implementation of our benchmark. Indeed, regardless of the input type of the benchmarked algorithm, the validation metrics are computed on a *fold* and never directly on the predicted and ground truth association matrices $(\hat{R}_{i,j}, A_{i,j})_{i \leq N_S, j \leq N_P}$. A fold is defined as a set of values referring to drug-disease pairs: *i.e.*, a set of indices $\mathcal{I} \subseteq \{1, 2, \dots, N_S\} \times \{1, 2, \dots, N_P\}$ such that the validation metric is computed on vectors $(\hat{R}_{i,j}, A_{i,j})_{(i,j) \in \mathcal{I}}$.

Moreover, at prediction time, matrix-oriented approaches can only provide predictions for drugs and diseases present in the matrix on which they have been trained. Suppose one needs to predict the outcome of a new drug-disease pair. In that case, one needs to concatenate information about this new drug or disease to the initial association matrix, run a training routine on this matrix again, and then make predictions. The same goes for supplementary information about drug-disease matches accrued after the initial training of the model. Consequently, this is potentially time-consuming and hinders drug repurposing of novel compounds.

Topic	Questions	Our recommendation
Evaluation of models	RQ1. Which metric should the model optimize for? RQ2. Which dataset should the model be evaluated on?	NS-AUC PREDICT (<i>private</i>) or DNdataset
Future models	RQ3. Should a method be pair- or matrix-oriented? RQ4. Which type of algorithms (MF, NN, GB) is the most promising?	Pair-oriented Graph-based

Table 4: Our guidelines for fairer and comprehensive benchmarks of collaborative-filtering-based drug repurposing models. MF: matrix factorization. NN: neural network. GB: graph-based.

2.4 Validation metrics for drug repurposing

As illustrated by Table 1, drug repurposing datasets are highly imbalanced and information-scarce, both between the known ($-1/+1$) and unknown (0) labels (column “sparsity”), and between the positive (+1) and negative (-1) associations (column “IR”). As such, a standard accuracy metric that only accounts for correct label predictions on known drug-disease associations is bound to be biased [3]. Moreover, only focusing on binary labels removes essential information about the ability of the model to rank drug-disease associations. We suggest several conditions to get the best interpretation out of a validation metric (in particular, for real-life applications). The metric should be bounded, ideally in the range $[0, 1]$, where 1 applies to a perfect drug repurposing model, 0 to a model which perfectly ranks *negative associations first*, and finally 0.5 for a ranking at random. See Table 3 for a few examples of standard metrics that satisfy these constraints. Moreover, in the application of drug repurposing, given that some diseases are investigated more than others, there is a discrepancy in the amount of information available on diseases. This is why we distinguish in Table 3 between “global” metrics, computed across all associations, and “local” ones, which average the metric obtained on disease-specific associations. As we will show in our benchmark in Section 3, models aiming at optimizing a global metric will not necessarily maximize a local metric.

As a consequence, we conjecture that a model that achieves a high global validation metric on a training set might provide a degraded prediction for a specific disease. This situation would not be satisfying for drug repurposing.

2.5 Quantifying robustness

In addition to the evaluation of the approximation error of a model—that is, how well the model retrieves known drug-disease associations—one is also interested in quantifying the robustness of the model and checking whether the model still performs well on data which is significantly dissimilar from the training data. This problem is pervasive in machine learning, particularly in health-related applications [8], where differences in technicians and measurement protocols can induce a shift in the distribution of values in the data. In prior works [13], this robustness was measured by training and testing a model on two datasets such that the Tanimoto score between one drug in the training set and another drug in the testing set is at most equal to 0.8.

In our benchmark, we generalize this procedure to other data types than structural fingerprints by splitting in an automated dataset into *weakly correlated* subsets depending on the drug similarity, as described in Section 5. This procedure allows us to have a proxy of the error induced by the distribution shift between the training and testing sets.

3 Results

We ran $N = 100$ iterations of each algorithm in Table 2 on each dataset in Table 1, and collected all metrics present in Table 3 as computed on the testing subset (20% of the total dataset) with the best model selected through a 5-fold cross validation on the training subset. The best model is the one that achieves the highest value of AUC across all five folds. Unless otherwise specified, a dataset is randomly split into training and testing sets containing disjoint drug-disease pairs. For further details about the setting of the benchmark, please refer to Section 5. Figure 2(a) shows a summary of the benchmarking pipeline. We summarize our insights from the benchmark in Table 4, highlighting the main research questions and our suggestions for tackling each of them. Figure 3 is the crucial result of the benchmark and shows the Top-3 contenders (in terms of average testing accuracy metric) for each dataset. We first consider questions regarding the evaluation of the drug repurposing performance.

3.1 Optimizing for AUC does not guarantee good disease-wise, nor ranking performance

We chose to perform model selection based on optimizing the (global) AUC, as done in many prior works [13, 32]. Figure 2(b) compares the distribution of the different metrics in Table 3. Unsurprisingly, as the models run on the testing subsets are selected based on their AUC value on the validation subset (part of the training subset), the AUC and accuracy values obtained on the testing subsets are overall relatively high. However, as illustrated by the diagonal plots and correlation values in Figure 2(b),

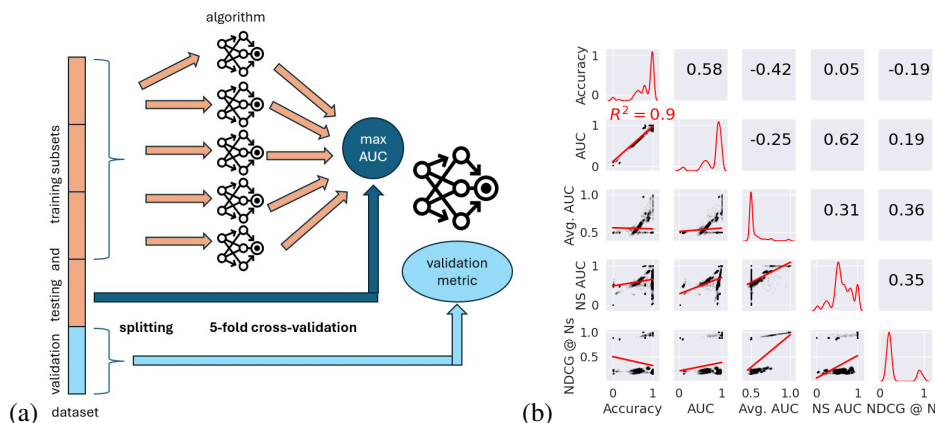


Figure 2: (a). Benchmarking training and testing pipeline iterated $N = 100$ times for drug repurposing for a specific algorithm, a splitting method for training/testing and validation subsets, and a validation metric. Note that the training/testing subsets are always split at random. (b). Correlogram of metrics collected during the benchmark on randomly split training and testing sets, referring to metrics in Table 3. The total number of considered values is then $N = 18,700$ (see Table 14 in Appendix). The lower triangle of the plot shows linear regressions between each pair of metrics, with the corresponding R^2 when greater than 0.25. The upper triangle displays the Spearman’s ρ correlations between each pair of metrics. The diagonal shows the empirical frequency distribution of values for each metric.

Synthetic	LRSSL	Gottlieb	Cdataset	Fdataset	PREDICT (<i>public</i>)	PREDICT	DNdataset	TRANSCRIPT
1.00	0.87	0.84	0.84	0.81	0.79	0.78	0.73	0.68

Table 5: Median NS–AUC value across Top-3 algorithms (in average) and all $N = 100$ iterations for each dataset in Table 1. The values are rounded up to the closest second decimal place.

AUC is only weakly positively correlated to local metrics (average AUC, average NS–AUC) and ranking metrics ($\text{NDCG}@N_S$). This is also illustrated in Figures 3 where the Top-3 algorithms in average testing AUC often differ from those computed based on average NS–AUC values (in 12 out of 16 comparisons). In the context of drug repurposing, the typical use case is to consider a disease for which treatments are missing (*e.g.*, in rare diseases) or no longer as effective (*e.g.*, in refractory epilepsies) and predict new therapeutic indications for this disease from a drug library. The first answer to RQ1 in Table 4 (“Which metric should the model optimize for?”) would be NS–AUC. On the other hand, users of a drug repurposing method might also be interested in a good ranking performance, as typically, several drug candidates will be outputted and checked in decreasing order of the associated scores. In that case, the answer to RQ1 would be $\text{NDCG}@N_S$.

3.2 Negative-Sampling AUC (NS–AUC) is a good measure of the performance of a model

[62] introduced what we call the “negative-sampling AUC” metric, which corresponds to the percentage of the natural order of associations (positive associations first, negative ones last, separated by unknown pairs) which is preserved by a classifier. The full expression of this metric is displayed in Table 3. Compared to the ranking measure $\text{NDCG}@N_S$, the NS–AUC has the advantage of being more strongly positively correlated with a global performance on known and unknown pairs (accuracy and “global” AUC values), as exemplified by Figure 2(b). Ultimately, the answer we recommend to Question 1 is to optimize for NS–AUC when training a drug repurposing model, as it fits the drug repurposing use case and obtains good performance for other validation metrics. Based on this recommendation, we focus on NS–AUC values to draw our conclusions in the remainder of this paper.

3.3 There is a need for more diverse reference drug repurposing datasets

The next question in Table 4 is “Which dataset should the model be evaluated on?”. In a benchmark of drug repurposing approaches, a reference dataset should feature data types that can be retrieved from public databases in a real-life application and be challenging enough to discriminate between drug repurposing algorithms. To quantify the difficulty associated with a dataset, we computed the median NS–AUC value across the Top-3 algorithms in average and all $N = 100$ iterations for this specific dataset. We focused on the top-3 contenders to determine a proper baseline for the performance expected on this dataset. The datasets are ranked according to these resulting scores in Table 5. As a sanity check, the synthetic dataset that we have built is

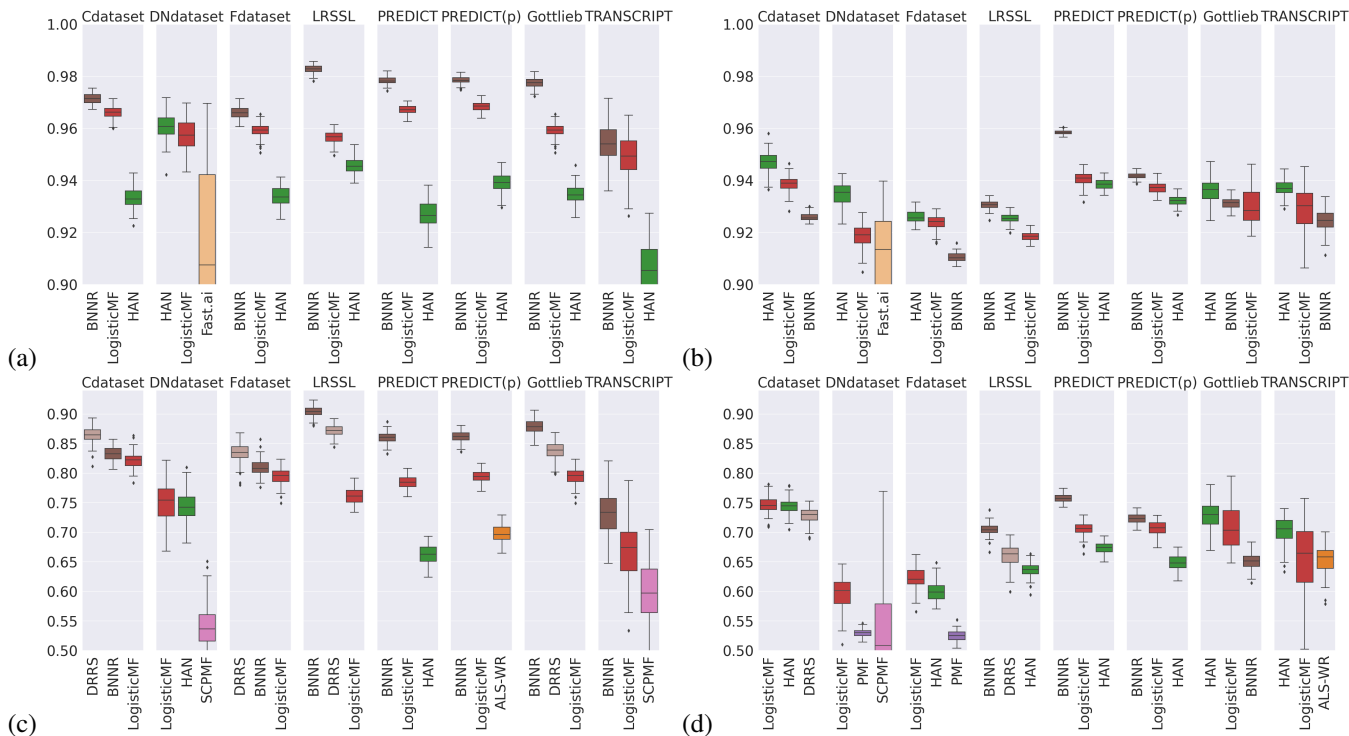


Figure 3: Boxplots of testing metric values for the Top-3 algorithms (in average) across $N = 100$ iterations for each dataset in Table 1, for a specific training/testing set splitting method. PREDICT(p) corresponds to the public version of PREDICT, whereas PREDICT refers to the private version of the dataset. (a) AUC values for randomly split sets. (b) AUC values for weakly correlated sets. (c) NS-AUC values for randomly split sets. (d) NS-AUC values for weakly correlated sets.

indeed very easy, as more than 50% of the time, the best algorithms on this dataset achieve perfect predictive power. The most frequent datasets present in the literature (LRSSL [27, 12], Cdataset, Fdataset [31]) also come at the top of this ranking, which seem unsurprising as most of the state-of-the-art algorithms which we have considered in the benchmark were trained (and probably finetuned) on these datasets. More interestingly, as described in Section 2, those datasets share the same types of data, namely, drug-disease associations from DrugBank, drug-pairwise chemical structure similarities, and disease-pairwise semantic similarities. This might explain why, even if they haven’t been tested on all of these “silver standard” datasets, state-of-the-art algorithms generally perform well on these. However, the DNdataset featuring drug annotation codes and disease ontologies, along with the newer PREDICT and TRANSCRIPT datasets with supplementary information from transcriptomics and regulatory networks, is a lot more challenging, as evidenced by the apparent drop in the ranking score. Then, we consider that the new challenge in drug repurposing is to beat the state-of-the-art on these three datasets.

3.4 Biological data-based drug and disease features are predictive of drug-disease associations

However, perhaps these three datasets have low ranking scores in Table 5 because the corresponding drug and disease features are not predictive of the drug-disease associations, hence inducing into error most of the drug repurposing algorithms. To test this theory on these three datasets, we used a (non-parametric) Kruskal-Wallis H-test to check whether the NS-AUC median value obtained with feature-agnostic algorithms was significantly different (and greater) than the NS-AUC median value obtained with algorithms that take into account drug and disease features. At significance level $\alpha = 1\%$ and adjusting p -values for multiple-tests with the Benjamini-Hochberg method [5], the test was significant for all of these three datasets: the TRANSCRIPT ($H = 26.5$), PREDICT (private version, $H = 50.0$), PREDICT (public, $H = 17.5$) and DNdataset ($H = 45.3$) datasets. Eventually, as mentioned in Table 4, we suggest the evaluation of drug repurposing methods on the private version of PREDICT (if the associated generating code can be run) or on the DNdataset which seem to be the most predictive of the drug-disease associations.

Dataset	Cdataset	LRSSL	PREDICT	DNdataset	TRANSCRIPT	Fdataset	PREDICT (<i>public</i>)	Gottlieb
H	26.4	43.0	70.8	84.1	97.3	128.5	143.2	144.1
$\mu_{\text{NN}} - \mu_{\text{GB}}$	-0.07	-0.06	-0.09	-0.21	-0.08	-0.11	-0.11	-0.11

Table 6: Results of Kruskal–Wallis H–tests for each dataset. For a fixed dataset d , the null hypothesis is “the median NS–AUC value $\mu_{\text{NN}}(d)$ obtained on dataset d by pair–oriented neural networks is equal to the median NS–AUC value $\mu_{\text{GB}}(d)$ on the same dataset by pair–oriented graph–based approaches”. In each test, the number of elements in each group is $N = 200$. The values are rounded up to the closest first or second decimal places. All tests on adjusted p –values are significant at level $\alpha = 1\%$.

3.5 As a general rule, matrix–oriented methods perform better

We now focus on developing future collaborative filtering approaches for drug repurposing. Across the top algorithms for average testing (global) AUC and NS–AUC values in Figure 3, the frequency of a pair–oriented algorithm being in the Top-3 is only $27/(4 \times 8 \times 3) \approx 28\%$, where the HAN algorithm [54] is the most frequent top pair–oriented method. This frequency decreases to 25% when considering only the top contender, whereas 36% of the algorithms in Table 2 are pair–oriented. Alas, the reason behind this is probably a certain amount of data leakage happening due to the structure of matrix–oriented methods, as described in Section 2. As such, even though this group of algorithms has good performances, we advise focusing on pair–oriented algorithms for Question 3 in Table 4.

3.6 General–purpose collaborative filtering algorithms remain competitive

Some of the algorithms present in Table 2 were not explicitly developed for drug repurposing but aimed to provide a generic recommender system for various goals, for instance, movie recommendation. As those algorithms are often ignored in drug repurposing–focused publications, we selected some general–purpose algorithms for the benchmark: based on matrix factorization approaches (ALS–WR, LibMF, LogisticMF, PMF) or embedding learning with neural networks (Fast.ai implementation of a collaborative learner). Our benchmark shows that those methods remain competitive for the drug repurposing problem, particularly LogisticMF, even if they are often not the top contender. As such, we advocate for including a comparable general–purpose recommender system when evaluating the performance of a drug repurposing algorithm.

3.7 Neural networks are noticeably better at generalizing

We observed the influence of weakly correlated training and testing subsets on the performance of models. From Figure 3, we expect that the difference in performance is vast between random and weakly correlated training and testing sets, independently from the validation metric and the algorithm. To confirm or infirm this assumption, we tested with a Kruskal–Wallis H test whether the median testing NS–AUC value across all datasets is significantly different for a specific type of algorithm (matrix factorization, neural networks, graph–based) on random splits compared to weakly correlated splits. It turns out that the difference in median values is significant at level $\alpha = 1\%$ (with p –values adjusted for multiple tests) for all types of algorithms and yields respective H–values 21.4, 308.5 and 1, 100.2 for neural networks, graph–based approaches, and matrix factorization methods. The lower the H–value is, the lesser the difference in performance when facing a testing subset weakly correlated to the training data. Unsurprisingly, neural networks are shown to have the most significant ability to generalize and be robust under data distribution shifts, which seems on par with observations from other research fields [52]. However, graph–based approaches come second.

3.8 Graph–based approaches perform best

Given our previous remarks, we restrict our comparison of algorithm types to pair–oriented methods. This automatically excludes matrix factorization approaches in our benchmark, according to Table 2. For each dataset, we want to determine whether a specific type of drug repurposing is noticeably better than the other. Similarly to our previous tests, we compare the median validation metric obtained by neural networks and graph–based approaches. The result table is shown in Table 6. Overall, graph–based approaches have a performance significantly superior to neural networks. We suppose that since most of these graph–based approaches aim to reconstruct a graph connecting drugs and diseases (including edges between pairs of drugs or diseases), these methods might be able to uncover some form of reasoning behind a given drug–disease association. Since graph–based methods have some ability to generalize, we recommend developing further the idea of completing drug–disease heterogeneous graphs for drug repurposing.

4 Discussion

To better understand the current landscape in collaborative filtering–based drug repurposing, we developed a benchmark of the 11 algorithms present in Table 2 on several diverse datasets shown in Table 1. We focused on the validation metrics mentioned in Table 3. This extensive benchmark allowed us to answer important questions about the proper development and evaluation of such models, especially related to their end goal: drug repurposing. Overall, we showed that specific care should be brought to the design and testing of drug repurposing models, as mistakes might lead to biased evaluations. We suggest developing further graph-based methods, which are promising according to our benchmark. We hope that those contributions and insights will further improve the development and the real-life application of drug repurposing approaches.

We have identified several future works of interest in this field of research. First, in addition to the prediction of novel drug–disease associations, an application in practice for medical purposes needs the implementation of accountability, meaning that further arguments beyond a simple score should be provided to justify a predicted positive association. The increase in the research related to interpretable or explainable machine learning is a step toward tackling this issue. Moreover, actual prediction scores can rank and prioritize specific drug–disease associations but do not represent a probability or an actual meaningful quantification of the strength of the association. Being able to quantify accurately and control for errors in false positive associations, for instance, is another important venue for research, related to the problem of calibration [10]. Finally, the problem of missing values is pervasive in many research fields, and biology is no exception. Whether imputation methods should be specific to biological data types is an interesting question, especially in the context of preserving interpretability and good calibration.

5 Methods

We describe in this section supplementary details about the benchmark and the statistical tests applied in Section 3.

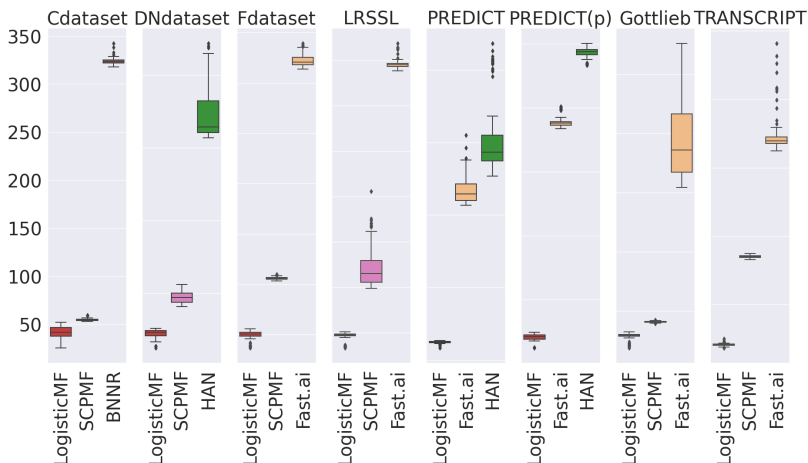


Figure 4: Training times in seconds across $N = 100$ iterations for each dataset and the fastest three algorithms among the most frequent Top-3 reported in Figure 3.

Selection of state-of-the-art algorithms We have considered drug repurposing algorithms from the recent literature (less than 8-year-old), which were: 1. based on collaborative filtering, 2. using as input only three matrices, as described in Section 2, 3. implemented and their code available in open–source or in a readily executable binary file. As such, all algorithms that we considered were run with their original implementation in R, MATLAB/Octave, or Python. In some cases, they encountered errors during their run. Please refer to the benchmark status in Table 14. A reimplemention in pure Python would probably fix these errors. However, this work is out of the scope of our paper. We also report in Figure 4 for each dataset the boxplots of training times (*i.e.*, the time to perform a 5-fold cross-validation) for the fastest three algorithms among those reported in at least two Top-3 in Figure 3.

The prediction times (*i.e.*, the time to generate scores on the 20% remaining drug–disease associations) are of the order of the second on all datasets and most algorithms. The exceptions are Fast.ai [20] and NIMCGCN [26], where the maximum prediction time across iterations and datasets is at most 50 seconds.

Processing of missing data in the benchmark Missing data refers here to unknown values in drug and disease feature matrices S and P , and occurs in dataset PREDICT (in the private version, 22% of drug feature values are missing in S , and

around 83% in P). To deal with this, for any dataset and any algorithm, each missing feature is imputed by the average value across the corresponding line (that is, other values for the same feature type across the dataset), and then standard-centered with classes `SimpleImputer` and `StandardScaler` in scikit-learn [37] before training a model.

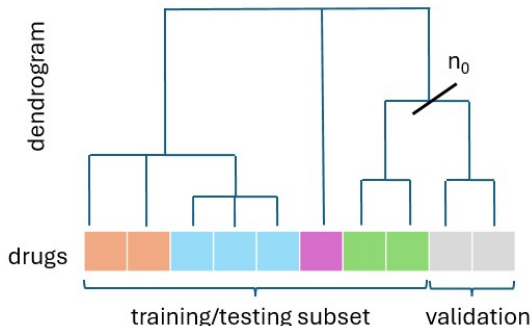


Figure 5: Illustration of the “weakly correlated” splitting approach to obtain training and validation subsets from a dataset.

Weakly correlated splits We introduced a simple procedure that generalizes the principle of assessing the predictive power of a model on novel drugs, dissimilar to the ones present in the training subset [13]. In prior works, authors chose a simple thresholding criterion, where drugs present in training and testing subsets have a Tanimoto similarity score on chemical structures at most 0.80.

Given a parameter $s \in (0, 1)$ corresponding to the desired percentage of associations in the training set, our procedure automatically splits the dataset of associations into two subsets such that the cosine similarity (by default) in a pair of drugs from different subsets is small. Our algorithm leverages a dendrogram built from a hierarchical clustering (with average linkage) applied to the drug feature vectors. Then, the procedure identifies with binary search the number of clusters n_0 , $2 \leq n_0 \leq N_S$, such that there exists a cluster identifier $c_0 \leq n_0$

$$|\{(d, p) \in A \mid \text{Clust}(d) \leq c\}| \approx (1 - s)N_S N_F ,$$

where Clust is the function that assigns to a drug its cluster identifier in $\{1, 2, \dots, n_0\}$. In Figure 5, the corresponding number of clusters for $s = 80\%$ is $n_0 = 5$ and $c_0 = 4$.

This procedure has a cubic time and memory computational complexity in the number of drugs in the worst case. In practice, for the small drug repurposing datasets in this paper, the computational cost of this procedure is negligible compared to the training phase.

Model	NS AUC	AUC
HAN	1.00 ± 0.0	1.00 ± 0.0
BNNR	1.00 ± 0.0	1.00 ± 0.0
LogisticMF	1.00 ± 0.0	1.00 ± 0.0
ALSWR	1.00 ± 2.10^{-6}	1.00 ± 1.10^{-3}
Fast.ai	1.00 ± 1.10^{-2}	1.00 ± 1.10^{-3}
LibMF	–	0.95 ± 9.10^{-4}
PMF	0.99 ± 2.10^{-3}	0.93 ± 4.10^{-3}
SCPMF	0.88 ± 2.10^{-1}	–
NIMCGCN	0.54 ± 4.10^{-3}	0.94 ± 5.10^{-4}

Table 7: The average \pm standard deviation validation metric on the randomly selected testing subset across $N = 100$ iterations for the Top-10 algorithms on the “Synthetic” dataset in Table 1. Average (resp., standard deviation) values are rounded to the closest second (resp., first) decimal place.

Model	NS AUC	AUC
HAN	1.00 ± 0.0	1.00 ± 0.0
Fast.ai	1.00 ± 0.0	1.00 ± 9.10 ⁻⁴
LogisticMF	0.99 ± 9.10 ⁻⁴	0.99 ± 1.10 ⁻⁴
BNNR	0.76 ± 3.10 ⁻³	0.98 ± 2.10 ⁻⁴
NIMCGCN	0.54 ± 3.10 ⁻⁴	0.97 ± 4.10 ⁻⁶
ALSWR	0.50 ± 0.0	—
LibMF	0.45 ± 1.10 ⁻¹⁶	0.98 ± 3.10 ⁻¹⁶
SCPMF	0.44 ± 7.10 ⁻²	0.40 ± 1.10 ⁻¹
LRSSL	—	0.15 ± 8.10 ⁻³
PMF	—	0.08 ± 7.10 ⁻³

Table 8: The average ± standard deviation validation metric on the weakly correlated testing subset across $N = 100$ iterations for the Top-10 algorithms on the ‘‘Synthetic’’ dataset in Table 1. Average (resp., standard deviation) values are rounded up to the closest second (resp., first) decimal place.

Synthetic dataset The synthetic dataset in Table 1 is the only dataset not directly available from the literature. It allows us to define a task with a controllable level of difficulty. In particular, the synthetic dataset in our benchmark should be an easy task on which all drug repurposing methods should perform excellently and provide a control for some statistical tests.

The generating function takes as input n_{pos} , the number of positive associations (+1’s in matrix A), n_{neg} , the number of negative associations (−1’s in matrix A), n_F , the even number of drug and disease features, and μ, σ the parameters from the Gaussian distribution of feature values. In practice, $\mu = 0.5$ and $\sigma = 1$. Then, we draw each feature value independently and identically (iid) from two Gaussian distributions of mean μ and $-\mu$ and variance σ^2 . That is, for any drug or disease $j \leq n_{\text{pos}}, n_{\text{neg}}$ and feature $i \leq n_F$:

$$X_{\text{pos}}[i, j] \sim_{\text{iid}} \mathcal{N}(+\mu, \sigma) \text{ and } X_{\text{neg}}[i, j] \sim_{\text{iid}} \mathcal{N}(-\mu, \sigma).$$

From those matrices, we build the final dataset as follows. A is the matrix in $\{-1, 0, +1\}^{N_S \times N_P}$ with zeros everywhere except in the square $\{(i, j) \mid 0 \leq i, j \leq n_{\text{pos}} - 1\}$ where there is only +1, and in the square $\{(i, j) \mid n_{\text{pos}} \leq i, j \leq n_{\text{pos}} + n_{\text{neg}} - 1\}$, which only contains −1, and where $N_S = N_P = n_{\text{pos}} + n_{\text{neg}}$. Then

$$S = \begin{bmatrix} X_{\text{pos}}[0 : N_F - 1, :] \\ X_{\text{neg}}[0 : N_F - 1, :] \end{bmatrix} \text{ and } P = \begin{bmatrix} X_{\text{pos}}[N_F : n_F, :] \\ X_{\text{neg}}[N_F : n_F, :] \end{bmatrix},$$

where $N_F = n_F/Z$, and $M[k : l, :]$ is the matrix where only the rows $k, k + 1, \dots, l - 1$ to l (included) remain. Then, the difficulty of the underlying drug repurposing problem can be tuned by the parameters of the Gaussian distributions μ and σ . The larger $\mu > 0$ and the smaller σ , the easier the problem. See Table 7, resp. Table 8, for the resulting validation metrics on the Top-10 algorithms for random, resp. weakly correlated, training/validation splits.

Statistical information We report here the missing result tables corresponding to the two-tailed Kruskal–Wallis H–tests run from Section 3.

• **Predictive power of features in datasets TRANSCRIPT, PREDICT and DNdataset** Table 9 shows the result table for the corresponding Kruskal–Wallis H–tests. For a fixed dataset d , the null hypothesis is ‘‘the median NS–AUC value $\mu_{\text{wf}}(d)$ obtained on dataset d by feature-aware methods is equal to the median NS–AUC value $\mu_{\text{wof}}(d)$ on the same dataset by feature-oblivious approaches. In each test, the number of elements in each group is $N = 600$. The values are rounded up to the closest first or second decimal places. The level of significance is $\alpha = 1\%$.

Dataset	A	B	C	D
H	26.5	17.5	50.0	45.3
adjusted p	0.0	3.10 ⁻⁶	0.0	0.0
$\mu_{\text{wf}} - \mu_{\text{wof}}$	0.07	0.12	0.12	0.14

Table 9: Kruskal–Wallis H–tests on the predictive power of features in datasets A=TRANSCRIPT, PREDICT (B=public and C=private versions) and D=DNdataset. The significance level is set to 1%, and p –values are adjusted for multiple tests with the Benjamini–Hochberg method [5]. All tests are statistically significant.

• **Generalization power of algorithm types** For a given algorithm type t , the null hypothesis is “the median NS–AUC value $\mu_{t,\text{Rand}}$ obtained by algorithms of type t on randomly split training/validation subsets is equal to the median NS–AUC value $\mu_{t,\text{WC}}$ on weakly correlated subsets. The values are rounded up to the closest first or second decimal places. The level of significance is $\alpha = 1\%$. In Table 10, N_{Rand} , resp. N_{WC} , is the number of samples in the “random”, resp. “weakly correlated”, group of validation metrics.

Type	GB	MF	NN
H	308.5	1100.2	21.4
adjusted p	0.0	0.0	4.10^{-6}
$\mu_{t,\text{Rand}} - \mu_{t,\text{WC}}$	0.10	0.15	0.02
N_{Rand}	2,500	4,600	1,700
N_{WC}	2,500	4,600	1,800

Table 10: Kruskal–Wallis H–tests on the generalization power of algorithm types “matrix factorization” (MF), “neural networks” (NN) and “graph–based” (GB) across datasets. The significance level is set to 1%, and p –values are adjusted for multiple tests with the Benjamini–Hochberg method [5]. All tests are statistically significant.

Model	Hyperparameter	Value
ALSWR	reg	0.01
	alpha	15
	n_iters	15
	n_factors	15
LibMF	fun	0
	k	8
	nr_bins	26
	n_iters	20
	lambda_p1	0.04
	lambda_p2	0.0
	lambda_q1	0.04
	lambda_q2	0.0
	eta	0.1
do_nmf	False	
LogisticMF	num_factors	2
	reg_param	0.6
	gamma	1.0
	iterations	30
PMF	reg	0.01
	learning_rate	0.1
	n_iters	160
	n_factors	15
	batch_size	100
SCPMF	r	15

Table 11: Hyperparameters of matrix factorization algorithms.

Hyperparameter tuning We considered for each algorithm the parameters provided in experiments in their current implementation, as, first, most were tested on the text–mining datasets in Table 1 and we aimed to reproduce their results; second, we wanted an evaluation of their performance in “real–life conditions” of drug repurposing, where the hyperparameter tuning is unlikely to be thorough. We were also wary of introducing further data leakage into the benchmark, especially, as the considered drug repurposing datasets are quite small. For general–purpose algorithms, we tune hyperparameters to corresponding values in drug repurposing algorithms, when possible (for instance, the learning rate or the embedding dimension). We report in Tables 13, 11 and 12 below the hyperparameter configurations for each algorithm across all datasets and iterations. We use the same parameter names as in the implementation in the `benchscofi` package [44].

Model	Hyperparameter	Value
Fast.ai	n_iterations	5
	n_factors	20
	weight_decay	0.1
	learning_rate	0.005
NIMCGCN	epoch	10
	alpha	10
	fg	256
	fd	256
	k	32
	learning_rate	0.001

Table 12: Hyperparameters of neural networks.

Model	Hyperparameter	Value
BNNR	maxiter	300
	alpha	1
	beta	10
	tol1	0.002
	tol2	1.10^{-5}
DRRS	–	–
HAN	k	15
	learning_rate	0.001
	epoch	1000
	weight_decay	0.0
LRSSL	k	10
	mu	0.01
	lam	0.01
	gam	2
	tol	0.01
	maxiter	500

Table 13: Hyperparameters of graph-based approaches.

Computational resources The experiments were run on remote cluster servers of Inria Saclay (processor QEMU Virtual v2.5+, 48 cores @2.20GHz, RAM 500GB) and SBI Rostock (processor Intel Core i7-8750H, 20 cores @2.50GHz, RAM 7.7GB). The clusters of Inria Saclay were favored for pure Python drug repurposing algorithms, whereas the server of SBI Rostock ran the other types of experiments. No GPU was used during the benchmark.

Benchmark status Table 14 displays the status of each runs of 100 iterations for each algorithm and dataset in the benchmark.

Dataset	Split	ALSWR	LibMF	LogisticMF	PMF	SCPMF	Fast.ai	NIMCGCN	BNNR	DRRS	HAN	LRSSL
Cdataset	random	✓	✓	✓	✓	✓	✓	✓	✓	✓	✓	✓
	weakly c.	✓	✓	✓	✓	✓	✓	✓	✓	✓	✓	✓
Fdataset	random	✓	✓	✓	✓	✓	✓	✓	✓	✓	✓	✓
	weakly c.	✓	✓	✓	✓	✓	✓	✓	✓	✓	✓	✓
DNdataset	random	× (M)	✓	✓	✓	✓	✓	× (M)	× (M)	× (M)	✓	✓
	weakly c.	× (M)	✓	✓	✓	✓	✓	✓	× (M)	× (M)	✓	✓
Gottlieb	random	✓	✓	✓	✓	✓	✓	✓	✓	✓	✓	✓
	weakly c.	✓	✓	✓	✓	✓	✓	✓	✓	✓	✓	✓
LRSSL	random	✓	✓	✓	✓	✓	✓	✓	✓	✓	✓	✓
	weakly c.	✓	✓	✓	✓	✓	✓	✓	✓	✓	✓	✓
PREDICT (private)	random	✓	✓	✓	✓	× (E)	✓	✓	✓	× (E)	✓	✓
	weakly c.	✓	✓	✓	✓	× (E)	✓	✓	✓	× (E)	✓	✓
PREDICT (public)	random	✓	✓	✓	✓	× (E)	✓	✓	✓	× (E)	✓	✓
	weakly c.	✓	✓	✓	✓	× (E)	✓	✓	✓	× (E)	✓	✓
TRANSCRIPT	random	✓	✓	✓	✓	✓	✓	✓	✓	× (E)	✓	× (E)
	weakly c.	✓	✓	✓	✓	✓	✓	✓	✓	× (E)	✓	× (E)
Synthetic	random	✓	✓	✓	✓	✓	✓	✓	✓	× (E)	✓	✓
	weakly c.	✓	✓	✓	✓	✓	✓	✓	✓	× (E)	✓	✓

Table 14: Report of the benchmark status across datasets and algorithms. ✓ means that the 100 iterations were successfully run, whereas × indicates an error (M: memory, E: runtime error).

References

- [1] Rishabh Agarwal, Max Schwarzer, Pablo Samuel Castro, Aaron C Courville, and Marc Bellemare. Deep reinforcement learning at the edge of the statistical precipice. *Advances in neural information processing systems*, 34:29304–29320, 2021.
- [2] Michael Ashburner, Catherine A Ball, Judith A Blake, David Botstein, Heather Butler, J Michael Cherry, Allan P Davis, Kara Dolinski, Selina S Dwight, Janan T Eppig, et al. Gene ontology: tool for the unification of biology. *Nature genetics*, 25(1):25–29, 2000.
- [3] Mohamed Bekkar, Hassiba Kheliouane Djemaa, and Taklit Akrouf Alitouche. Evaluation measures for models assessment over imbalanced data sets. *J Inf Eng Appl*, 3(10), 2013.
- [4] Bell, Koren, and Volinsky. Modeling relationships at multiple scales to improve accuracy of large recommender systems. In *Proceedings of the 13th ACM SIGKDD*, 2007.
- [5] Yoav Benjamini and Yosef Hochberg. Controlling the false discovery rate: a practical and powerful approach to multiple testing. *Journal of the Royal statistical society: series B (Methodological)*, 57(1):289–300, 1995.
- [6] S Bala Bhaskar. Concealing research outcomes: Missing data, negative results and missed publications. *Indian Journal of Anaesthesia*, 61(6):453, 2017.
- [7] Adam S Brown and Chirag J Patel. A standard database for drug repositioning. *Scientific data*, 4(1):1–7, 2017.
- [8] Adam M Chekroud, Matt Hawrilenko, Hieronimus Loho, Julia Bondar, Ralitza Gueorguieva, Alkomiet Hasan, Joseph Kambeitz, Philip R Corlett, Nikolaos Koutsouleris, Harlan M Krumholz, et al. Illusory generalizability of clinical prediction models. *Science*, 383(6679):164–167, 2024.
- [9] Wei-Sheng Chin, Bo-Wen Yuan, Meng-Yuan Yang, Yong Zhuang, Yu-Chin Juan, and Chih-Jen Lin. Libmf: a library for parallel matrix factorization in shared-memory systems. *Journal of Machine Learning Research*, 17(86):1–5, 2016.
- [10] William Fithian and Lihua Lei. Conditional calibration for false discovery rate control under dependence. *The Annals of Statistics*, 50(6):3091–3118, 2022.
- [11] Evelyn Fix. *Discriminatory analysis: nonparametric discrimination, consistency properties*, volume 1. USAF school of Aviation Medicine, 1985.
- [12] Chu-Qiao Gao, Yuan-Ke Zhou, Xiao-Hong Xin, Hui Min, and Pu-Feng Du. Dda-skf: Predicting drug–disease associations using similarity kernel fusion. *Frontiers in Pharmacology*, 12:784171, 2022.
- [13] Assaf Gottlieb, Gideon Y Stein, Eytan Ruppim, and Roded Sharan. Predict: a method for inferring novel drug indications with application to personalized medicine. *Molecular systems biology*, 7(1):496, 2011.
- [14] Ada Hamosh, Alan F Scott, Joanna Amberger, David Valle, and Victor A McKusick. Online mendelian inheritance in man (omim). *Human mutation*, 15(1):57–61, 2000.
- [15] Tal Hassner and Itzik Bayaz. Teaching computer vision: Bringing research benchmarks to the classroom. *ACM Transactions on Computing Education (TOCE)*, 14(4):1–17, 2015.
- [16] Jieyue He, Xinxing Yang, Zhuo Gong, et al. Hybrid attentional memory network for computational drug repositioning. *BMC bioinformatics*, 21(1):1–17, 2020.
- [17] Aroon D Hingorani, Valerie Kuan, Chris Finan, Felix A Kruger, Anna Gaulton, Sandesh Chopade, Reecha Sofat, Raymond J MacAllister, John P Overington, Harry Hemingway, et al. Improving the odds of drug development success through human genomics: modelling study. *Scientific reports*, 9(1):18911, 2019.
- [18] Rachel A Hodos, Brian A Kidd, Shameer Khader, Ben P Readhead, and Joel T Dudley. Computational approaches to drug repurposing and pharmacology. *Wiley interdisciplinary reviews. Systems biology and medicine*, 8(3):186, 2016.
- [19] Rachel A Hodos, Brian A Kidd, Khader Shameer, Ben P Readhead, and Joel T Dudley. In silico methods for drug repurposing and pharmacology. *Wiley Interdisciplinary Reviews: Systems Biology and Medicine*, 8(3):186–210, 2016.
- [20] Howard et al. fastai. <https://github.com/fastai/fastai>, 2018.
- [21] Yu-Guan Hsieh, Gang Niu, and Masashi Sugiyama. Classification from positive, unlabeled and biased negative data. In *International Conference on Machine Learning*, pages 2820–2829. PMLR, 2019.

- [22] Christopher C Johnson et al. Logistic matrix factorization for implicit feedback data. *Advances in Neural Information Processing Systems*, 27(78):1–9, 2014.
- [23] Richard T Johnson and Kay Dickersin. Publication bias against negative results from clinical trials: three of the seven deadly sins. *Nature Clinical Practice Neurology*, 3(11):590–591, 2007.
- [24] Sayash Kapoor and Arvind Narayanan. Leakage and the reproducibility crisis in machine-learning-based science. *Patterns*, 4(9), 2023.
- [25] Andreas Köpf, Yannic Kilcher, Dimitri von Rütte, Sotiris Anagnostidis, Zhi Rui Tam, Keith Stevens, Abdullah Barhoum, Duc Nguyen, Oliver Stanley, Richárd Nagyfi, et al. Openassistant conversations-democratizing large language model alignment. *Advances in Neural Information Processing Systems*, 36, 2024.
- [26] Jin Li, Sai Zhang, Tao Liu, Chenxi Ning, Zhuoxuan Zhang, and Wei Zhou. Neural inductive matrix completion with graph convolutional networks for mirna-disease association prediction. *Bioinformatics*, 36(8):2538–2546, 2020.
- [27] Xujun Liang, Pengfei Zhang, Lu Yan, Ying Fu, Fang Peng, Lingzhi Qu, Meiyong Shao, Yongheng Chen, and Zhuchu Chen. Lrssl: predict and interpret drug–disease associations based on data integration using sparse subspace learning. *Bioinformatics*, 33(8):1187–1196, 2017.
- [28] Dekang Lin et al. An information-theoretic definition of similarity. In *Icml*, volume 98, pages 296–304, 1998.
- [29] Hui Liu, Wenhao Zhang, Lixia Nie, Xiancheng Ding, Judong Luo, and Ling Zou. Predicting effective drug combinations using gradient tree boosting based on features extracted from drug-protein heterogeneous network. *BMC bioinformatics*, 20(1):1–12, 2019.
- [30] Chuan Luo, Pu Zhao, Chen Chen, Bo Qiao, Chao Du, Hongyu Zhang, Wei Wu, Shaowei Cai, Bing He, Saravanakumar Rajmohan, et al. Pulns: Positive-unlabeled learning with effective negative sample selector. In *Proceedings of the AAAI Conference on Artificial Intelligence*, volume 35, pages 8784–8792, 2021.
- [31] Huimin Luo, Min Li, Shaokai Wang, Quan Liu, Yaohang Li, and Jianxin Wang. Computational drug repositioning using low-rank matrix approximation and randomized algorithms. *Bioinformatics*, 34(11):1904–1912, 2018.
- [32] Huimin Luo, Jianxin Wang, Min Li, Junwei Luo, Xiaoqing Peng, Fang-Xiang Wu, and Yi Pan. Drug repositioning based on comprehensive similarity measures and bi-random walk algorithm. *Bioinformatics*, 32(17):2664–2671, 2016.
- [33] Victor Martinez, Carmen Navarro, Carlos Cano, Waldo Fajardo, and Armando Blanco. Drugnet: network-based drug–disease prioritization by integrating heterogeneous data. *Artificial intelligence in medicine*, 63(1):41–49, 2015.
- [34] Matthew McDermott, Shirly Wang, Nikki Marinsek, Rajesh Ranganath, Marzyeh Ghassemi, and Luca Foschini. Reproducibility in machine learning for health. *arXiv preprint arXiv:1907.01463*, 2019.
- [35] Yajie Meng, Min Jin, Xianfang Tang, and Junlin Xu. Drug repositioning based on similarity constrained probabilistic matrix factorization: Covid-19 as a case study. *Applied soft computing*, 103:107135, 2021.
- [36] Gang Niu, Marthinus Christoffel du Plessis, Tomoya Sakai, Yao Ma, and Masashi Sugiyama. Theoretical comparisons of positive-unlabeled learning against positive-negative learning. *Advances in neural information processing systems*, 29, 2016.
- [37] Fabian Pedregosa, Gaël Varoquaux, Alexandre Gramfort, Vincent Michel, Bertrand Thirion, Olivier Grisel, Mathieu Blondel, Peter Prettenhofer, Ron Weiss, Vincent Dubourg, et al. Scikit-learn: Machine learning in python. *the Journal of machine Learning research*, 12:2825–2830, 2011.
- [38] Alex Philippidis. The unbearable cost of drug development: Deloitte report shows 15% jump in r&d to \$2.3 billion: A separate study published by british researchers shows biopharma giants spent 57% more on operating costs than research from 1999-2018. *GEN Edge*, 5(1):192–198, 2023.
- [39] Sudeep Pushpakom, Francesco Iorio, Patrick A Eyers, K Jane Escott, Shirley Hopper, Andrew Wells, Andrew Doig, Tim Williams, Joanna Latimer, Christine McNamee, et al. Drug repurposing: progress, challenges and recommendations. *Nature reviews Drug discovery*, 18(1):41–58, 2019.
- [40] Clémence Réda. Drug repurposing datasets for collaborative filtering methods (2.0.0), 2023. Notebooks.
- [41] Clémence Réda. Predict drug repurposing dataset (2.0.1), 2023. Dataset.

- [42] Clémence Réda. Transcript drug repurposing dataset (2.0.0), 2023. Dataset.
- [43] Clémence Réda, Jill-Jënn Vie, and Olaf Wolkenhauer. A new standard for drug repurposing by collaborative filtering: stanscofi and benchscofi. 2023.
- [44] Clémence Réda, Jill-Jënn Vie, and Olaf Wolkenhauer. stanscofi and benchscofi: a new standard for drug repurposing by collaborative filtering. *Journal of Open Source Software*, 9(93):5973, 2024.
- [45] Steffen Rendle. Factorization machines. In *2010 IEEE International conference on data mining*, pages 995–1000. IEEE, 2010.
- [46] Steffen Rendle, Christoph Freudenthaler, Zeno Gantner, and Lars Schmidt-Thieme. Bpr: Bayesian personalized ranking from implicit feedback. *arXiv preprint arXiv:1205.2618*, 2012.
- [47] Lynn Marie Schriml, Cesar Arze, Suvarna Nadendla, Yu-Wei Wayne Chang, Mark Mazaitis, Victor Felix, Gang Feng, and Warren Alden Kibbe. Disease ontology: a backbone for disease semantic integration. *Nucleic acids research*, 40(D1):D940–D946, 2012.
- [48] Francesca Spezzano, Wei Chen, and Xiaokui Xiao. *Proceedings of the 2019 IEEE/ACM International Conference on Advances in Social Networks Analysis and Mining*. ACM, 2019.
- [49] Aravind Subramanian, Rajiv Narayan, Steven M Corsello, David D Peck, Ted E Natoli, Xiaodong Lu, Joshua Gould, John F Davis, Andrew A Tubelli, Jacob K Asiedu, et al. A next generation connectivity map: L1000 platform and the first 1,000,000 profiles. *Cell*, 171(6):1437–1452, 2017.
- [50] Duxin Sun, Wei Gao, Hongxiang Hu, and Simon Zhou. Why 90% of clinical drug development fails and how to improve it? *Acta Pharmaceutica Sinica B*, 12(7):3049–3062, 2022.
- [51] Gábor Takács, István Pilászy, Bottyán Németh, and Domonkos Tikk. Matrix factorization and neighbor based algorithms for the netflix prize problem. In *Proceedings of the 2008 ACM conference on Recommender systems*, pages 267–274, 2008.
- [52] Rohan Taori, Achal Dave, Vaishaal Shankar, Nicholas Carlini, Benjamin Recht, and Ludwig Schmidt. Measuring robustness to natural distribution shifts in image classification. *Advances in Neural Information Processing Systems*, 33:18583–18599, 2020.
- [53] Dong Wang, Juan Wang, Ming Lu, Fei Song, and Qinghua Cui. Inferring the human microRNA functional similarity and functional network based on microRNA-associated diseases. *Bioinformatics*, 26(13):1644–1650, 2010.
- [54] Xiao Wang, Houye Ji, Chuan Shi, Bai Wang, Yanfang Ye, Peng Cui, and Philip S Yu. Heterogeneous graph attention network. In *The world wide web conference*, pages 2022–2032, 2019.
- [55] Zichen Wang, Caroline D Monteiro, Kathleen M Jagodnik, Nicolas F Fernandez, Gregory W Gundersen, Andrew D Rouillard, Sherry L Jenkins, Axel S Feldmann, Kevin S Hu, Michael G McDermott, et al. Extraction and analysis of signatures from the gene expression omnibus by the crowd. *Nature communications*, 7(1):12846, 2016.
- [56] David S Wishart, Craig Knox, An Chi Guo, Dean Cheng, Savita Shrivastava, Dan Tzur, Bijaya Gautam, and Murtaza Hassanali. Drugbank: a knowledgebase for drugs, drug actions and drug targets. *Nucleic acids research*, 36(suppl_1):D901–D906, 2008.
- [57] Mengyun Yang, Huimin Luo, Yaohang Li, and Jianxin Wang. Drug repositioning based on bounded nuclear norm regularization. *Bioinformatics*, 35(14):i455–i463, 2019.
- [58] Wanjuan Yang, Jorge Soares, Patricia Greninger, Elena J Edelman, Howard Lightfoot, Simon Forbes, Nidhi Bindal, Dave Beare, James A Smith, I Richard Thompson, et al. Genomics of drug sensitivity in cancer (gdsc): a resource for therapeutic biomarker discovery in cancer cells. *Nucleic acids research*, 41(D1):D955–D961, 2012.
- [59] Xinxing Yang, Genke Yang, and Jian Chu. The computational drug repositioning without negative sampling. *IEEE/ACM Transactions on Computational Biology and Bioinformatics*, 2022.
- [60] Xinxing Yang, Genke Yang, and Jian Chu. Self-supervised learning for label sparsity in computational drug repositioning. *IEEE/ACM Transactions on Computational Biology and Bioinformatics*, 2023.
- [61] Xinxing Yang, Ibrahim Zamit, Yu Liu, and Jiyeue He. Additional neural matrix factorization model for computational drug repositioning. *BMC bioinformatics*, 20:1–11, 2019.

[62] Hsiang-Fu Yu, Mikhail Bilenko, and Chih-Jen Lin. Selection of negative samples for one-class matrix factorization. In *Proceedings of the 2017 SIAM International Conference on Data Mining*, pages 363–371. SIAM, 2017.

[63] Deborah A Zarin, Tony Tse, Rebecca J Williams, Robert M Califf, and Nicholas C Ide. The clinicaltrials.gov results database—update and key issues. *New England Journal of Medicine*, 364(9):852–860, 2011.

6 Acknowledgements

This work was completed during a secondment of C.R. at Soda Team, Inria Saclay, F-91120 Palaiseau, France. The research leading to these results has received funding from the European Union’s HORIZON 2020 Programme under grant agreement no. 101102016 (RECeSS, HORIZON TMA MSCA Postdoctoral Fellowships - European Fellowships, C.R.). The funding sources have played no role in the design, the execution nor the analyses performed in this study.

7 Author contributions

C.R. has designed the study, implemented the tools and wrote the draft of the manuscript. J.-J.V. and O.W. substantially contributed to the writing and revision of the manuscript.

8 Data availability statement

Datasets & algorithms In addition to repositories mentioned in the publications in which they were introduced, all the datasets mentioned in Table 1 and drug repurposing algorithms in Table 2 are publicly available through the open-source Python packages `stanscofi` (version 2.0.1) and `benchcofi` (version 2.0.0) [44] which can be downloaded from the Python Package Index (PyPI). The only exception is the private version of PREDICT, which cannot be shared freely due to copyright issues with some of the databases on which it was built [41]. Nonetheless, this dataset can be built from scratch from Jupyter notebooks in the following GitHub repository:

[RECeSS-EU-Project/drug-repurposing-datasets](https://github.com/RECeSS-EU-Project/drug-repurposing-datasets)

Benchmark traces The results (metrics and runtimes) obtained on each successful iteration of the algorithms and datasets in this benchmark are stored in this GitHub repository:

[RECeSS-EU-Project/benchmark-results](https://github.com/RECeSS-EU-Project/benchmark-results)

Code availability The implementation of the benchmark pipeline and analysis scripts is publicly available at the following GitHub repository:

[RECeSS-EU-Project/benchmark-code](https://github.com/RECeSS-EU-Project/benchmark-code)

After installation and running the benchmark (corresponding instructions are present in the description of the repository), the script generating the figures and the statistical tests in Section 3 can be run with the following command

```
python3 -m analyses
```

9 Additional Information

The authors declare no competing interests.

Figure legends

- 1 Principle of collaborative filtering. If two drugs A and B are similar, and if there is a known association between a disease and drug A, then the same association is predicted between this disease and drug B. 2

2	(a). Benchmarking training and testing pipeline iterated $N = 100$ times for drug repurposing for a specific algorithm, a splitting method for training/testing and validation subsets, and a validation metric. Note that the training/testing subsets are always split at random. (b). Correlogram of metrics collected during the benchmark on randomly split training and testing sets, referring to metrics in Table 3. The total number of considered values is then $N = 18,700$ (see Table 14 in Appendix). The lower triangle of the plot shows linear regressions between each pair of metrics, with the corresponding R^2 when greater than 0.25. The upper triangle displays the Spearman’s ρ correlations between each pair of metrics. The diagonal shows the empirical frequency distribution of values for each metric.	7
3	Boxplots of testing metric values for the Top-3 algorithms (in average) across $N = 100$ iterations for each dataset in Table 1, for a specific training/testing set splitting method. PREDICT(p) corresponds to the public version of PREDICT, whereas PREDICT refers to the private version of the dataset. (a) AUC values for randomly split sets. (b) AUC values for weakly correlated sets. (c) NS–AUC values for randomly split sets. (d) NS–AUC values for weakly correlated sets.	8
4	Training times in seconds across $N = 100$ iterations for each dataset and the fastest three algorithms among the most frequent Top-3 reported in Figure 3.	10
5	Illustration of the “weakly correlated” splitting approach to obtain training and validation subsets from a dataset.	11

Tables

1	Datasets in the benchmark. They correspond to the number of drugs and diseases involved in at least one nonzero drug-disease association. The sparsity s is the percentage of unknown (neither positive nor negative) matches times 100 over the total number of possible drug-disease matches (rounded up to the first decimal place). The imbalance ratio IR is the ratio between negative and positive outcomes in the dataset (rounded up to the second decimal place). The private version of PREDICT is the one generated from notebooks in the original GitHub repository, whereas the public one is the one deposited on Zenodo [41]. The association matrix in the Fdataset comes from [13]. Still, the drug and disease features are from [32].	3
2	Overview of algorithms present in the benchmark present in Section 5 and the classification (columns “Class” and “I/O type”) defined in Section 2.	4
3	Description of the considered validation metrics present in Section 5. $\Omega^\pm \triangleq \{(i, j), A[i, j] = \pm 1 \mid i \leq N_S, j \leq N_P\}$, whereas $\Omega_j^+ \triangleq \{i \mid A[i, j] = +1\}$ and $\tilde{\Omega}_j \triangleq \{(i, i') \mid A[i, j] > A[i', j]\}$ for any $j \leq N_P$. In the benchmark, $t = 0$ and $\mathbb{1}(C)$ is equal to 1 if C is satisfied, 0 otherwise. σ_V is the permutation that sorts all coefficients of any vector V of length n in decreasing order, that is, $V[\sigma_V(1)] \geq V[\sigma_V(2)] \geq \dots \geq V[\sigma_V(n)]$. The true positive rate is defined as $\text{TPR}(t; \hat{R}, A) = \sum_{(i,j), A[i,j]=+1} \mathbb{1}(\hat{R}_{i,j} > t) / \sum_{(i,j)} \mathbb{1}(\hat{R}_{i,j} > t)$ and $\text{FPR}(t; \hat{R}, A) = \sum_{(i,j), A[i,j]=-1} \mathbb{1}(\hat{R}_{i,j} > t) / \sum_{(i,j)} \mathbb{1}(\hat{R}_{i,j} \leq t)$ is the false positive rate. Finally, N_S^+ is defined as $\min(N_S, \Omega_j^+)$	5
4	Our guidelines for fairer and comprehensive benchmarks of collaborative-filtering-based drug repurposing models. MF: matrix factorization. NN: neural network. GB: graph-based.	6
5	Median NS–AUC value across Top-3 algorithms (in average) and all $N = 100$ iterations for each dataset in Table 1. The values are rounded up to the closest second decimal place.	7
6	Results of Kruskal–Wallis H–tests for each dataset. For a fixed dataset d , the null hypothesis is “the median NS–AUC value $\mu_{\text{NN}}(d)$ obtained on dataset d by pair-oriented neural networks is equal to the median NS–AUC value $\mu_{\text{GB}}(d)$ on the same dataset by pair-oriented graph-based approaches”. In each test, the number of elements in each group is $N = 200$. The values are rounded up to the closest first or second decimal places. All tests on adjusted p –values are significant at level $\alpha = 1\%$	9
7	The average \pm standard deviation validation metric on the randomly selected testing subset across $N = 100$ iterations for the Top-10 algorithms on the “Synthetic” dataset in Table 1. Average (resp., standard deviation) values are rounded to the closest second (resp., first) decimal place.	11
8	The average \pm standard deviation validation metric on the weakly correlated testing subset across $N = 100$ iterations for the Top-10 algorithms on the “Synthetic” dataset in Table 1. Average (resp., standard deviation) values are rounded up to the closest second (resp., first) decimal place.	12

9	Kruskal–Wallis H–tests on the predictive power of features in datasets A=TRANSCRIPT, PREDICT (B=public and C=private versions) and D=DNdataset. The significance level is set to 1%, and p –values are adjusted for multiple tests with the Benjamini–Hochberg method [5]. All tests are statistically significant.	12
10	Kruskal–Wallis H–tests on the generalization power of algorithm types “matrix factorization” (MF), “neural networks” (NN) and “graph–based” (GB) across datasets. The significance level is set to 1%, and p –values are adjusted for multiple tests with the Benjamini–Hochberg method [5]. All tests are statistically significant.	13
11	Hyperparameters of matrix factorization algorithms.	13
12	Hyperparameters of neural networks.	14
13	Hyperparameters of graph–based approaches.	14
14	Report of the benchmark status across datasets and algorithms. ✓ means that the 100 iterations were successfully run, whereas × indicates an error (M: memory, E: runtime error).	15